Evaluation of an AAV9-mini-dystrophin gene therapy candidate in a rat model of Duchenne muscular dystrophy

Caroline Le Guiner,[1,11] Xiao Xiao,[2,11] Thibaut Larcher,[3] Aude Lafoux,[4] Corinne Huchet,[1,4] Gilles Toumaniantz,[4,5] Oumeya Adjali,[1] Ignacio Anegon,[6] Séverine Remy,[6] Josh Grieger,[7] Juan Li,[8] Vahid Farrokhi,[9] Hendrik Neubert,[9] Jane Owens,[10] Maritza McIntyre,[7] Philippe Moullier,[1] and R. Jude Samulski[2]

[1]Nantes Université, CHU Nantes, INSERM, TaRGeT, UMR 1089, Translational Research for Gene Therapies, 44200 Nantes, France; [2]Gene Therapy Center, University of North Carolina, Chapel Hill, NC 27599-7352, USA; [3]INRAE Oniris, UMR 703, PanTher, APEX, 44307 Nantes, France; [4]Therassay Platform, Capacités, Nantes Université, 44007 Nantes, France; [5]Nantes Université, CHU Nantes, CNRS, L'Institut du Thorax, 44007 Nantes, France; [6]Nantes Université, CHU Nantes, INSERM, Center for Research in Transplantation and Translational Immunology, UMR 1064, ITUN, 44093 Nantes, France; [7]Bamboo Therapeutics, Pfizer, Chapel Hill, NC 27514, USA; [8]Gene Therapy Center, Eshelman School of Pharmacy DPMP, University of North Carolina, Chapel Hill, NC 27599-7352, USA; [9]Pfizer Inc., Andover, MA 01810, USA; [10]Pfizer Inc., Cambridge, MA 02139, USA

Duchenne muscular dystrophy (DMD) is an X-linked disease caused by loss-of-function mutations in the *dystrophin* gene and is characterized by muscle wasting and early mortality. Adeno-associated virus-mediated gene therapy is being investigated as a treatment for DMD. In the nonclinical study documented here, we determined the effective dose of fordadistrogene movaparvovec, a clinical candidate adeno-associated virus serotype 9 vector carrying a human mini-dystrophin transgene, after single intravenous injection in a dystrophin-deficient (DMD^mdx) rat model of DMD. Overall, we found that transduction efficiency, number of muscle fibers expressing the human mini-dystrophin polypeptide, improvement of the skeletal and cardiac muscle tissue architecture, correction of muscle strength and fatigability, and improvement of diastolic and systolic cardiac function were directly correlated with the amount of vector administered. The effective dose was then tested in older DMD^mdx rats with a more dystrophic phenotype similar to the pathology observed in older patients with DMD. Except for a less complete rescue of muscle function in the oldest cohort, fordadistrogene movaparvovec was also found to be therapeutically effective in older DMD^mdx rats, suggesting that this product may be appropriate for evaluation in patients with DMD at all stages of disease.

INTRODUCTION

Duchenne muscular dystrophy (DMD) is a recessive X-linked disease caused by mutations in the *DMD* gene encoding dystrophin.[1] DMD affects ~1 in 5,000 newborn boys.[2] Dystrophin is an intracellular protein that mechanically connects the cytoskeleton to the extracellular matrix via the dystrophin-glycoprotein complex.[3] It increases muscle cell plasma membrane integrity, which prevents membrane damage during contraction. Without dystrophin, myofibers suffer cellular damage, degeneration, and necrosis, resulting in progressive muscle weakness and wasting.[4,5] All muscles are affected, including the heart and respiratory muscles.[5–7] Patients generally exhibit muscle weakness beginning in early childhood and lose ambulation by ~10–12 years of age.[8] Life expectancy is severely shortened because of cardiac or respiratory failure, although use of respiratory support has extended patient lifespan into the mid-thirties.[6,7] Use of corticosteroids with physiotherapy, nutrition, and counseling have had a modest impact on the natural course of the disease.[7] Finally, although readthrough drugs and exon-skipping approaches can moderately improve levels of dystrophin with limited functional improvements,[9,10] there is currently no treatment that can fully compensate for the lack of functional dystrophin.

Restoring functional dystrophin would be a transformational therapy. One possible approach is delivery of a mini-dystrophin gene, body wide, with use of an adeno-associated virus (AAV) as a vector.[11] Recombinant AAV (rAAV) vectors have been used to establish long-term *in vivo* gene expression in a variety of tissues, including muscle, with superior gene transfer efficiency and longevity compared with other viral and non-viral vectors.[12,13] Because of their relatively small viral particle size (~20 nm), AAV vectors can readily cross extracellular barriers that impede larger viral and non-viral vectors.[12,14] However, the small size of AAV vectors limits the package size that can be delivered and only allows for genes of less than 5 kb, precluding the full native dystrophin cDNA, which is 14 kb.[15,16] This packaging limitation required development of AAV mini/micro-dystrophins less than 5 kb in size for use in gene therapy for DMD.[17–22]

Correspondence: R. Jude Samulski, Gene Therapy Center, University of North Carolina, Chapel Hill, NC, USA.
E-mail: rjs@med.unc.edu

Different rAAV vectors have been developed from different AAV serotypes, which initiate entry into cells through interactions between the AAV capsid and specific carbohydrates on the cell surface.[23,24] These interactions lead to preferential transduction of different cell types by each serotype of rAAVs.[24,25] Serotype rAAV9 vectors have been reported to transduce skeletal and cardiac muscle, tissues most affected in DMD.[25–27] Mini/micro-dystrophins using rAAV9 vectors have been successfully transduced in animal models of DMD, including dystrophin-deficient (*mdx*) mice, utrophin/dystrophin double knockout mice, and the golden retriever muscular dystrophy (GRMD) dog model.[16,17,21,27–32]

The DMD*^mdx^* rat has been characterized previously as a model of DMD.[33–36] The dystrophic phenotype in this model can be detected as soon as 10 days of age, with obvious pathologic features noted at 1.5 months that progress with advancing age. Specifically, DMD*^mdx^* rats have systematic and stepwise severe phenotypes in skeletal and cardiac muscle, similar to patients with DMD, and a reduced lifespan (mean age of survival is 12 months). This model also offers high phenotypic reproducibility and stability with little or no phenotypic variation between animals. Therefore, this model may be more suitable for preclinical evaluations than the original *mdx* mouse or GRMD dog models that have been widely used in preclinical evaluations of therapeutic products for DMD but that are characterized by late onset and inconsistent cardiac alterations.[37]

The purpose of this study was to determine the pharmacologically effective dose of fordadistrogene movaparvovec, an rAAV serotype 9 vector, expressing a human mini-dystrophin transgene (the transgene is described in Kornegay et al.[27]) under the control of a muscle-specific promoter that was administered intravenously to 2-month-old DMD*^mdx^* rats.[34] The effective dose determined in this study was then evaluated in older DMD*^mdx^* rats, which may mimic the evaluation in patients with more advanced disease.

RESULTS

Study design

A total of 90 DMD*^mdx^* rats and 26 wild-type (WT) rats were enrolled. Four vector-treated groups received 1×10^{13} vg/kg (vector genomes per kilogram of body weight), 3×10^{13} vg/kg, 1×10^{14} vg/kg, or 3×10^{14} vg/kg intravenously. Rats in the dose-range study (n = 66 DMD*^mdx^* and 14 WT) were assigned to treatment at ~2 months of age and sacrificed at 3 or 6 months post injection (p.i.). Some older rats (n = 24 DMD*^mdx^* and 12 WT) were also injected at 4 or 6 months of age and sacrificed at 3 months p.i. (Table 1). Age-matched vehicle-treated WT and vehicle-treated DMD*^mdx^* animals were used for comparison in each experiment (hereafter referred to as WT and DMD*^mdx^* controls). Moreover, a comprehensive pathological analysis was performed on groups of untreated DMD*^mdx^* rats euthanized at 2, 4, or 6 months of age, which were the ages at the time of vector administration to the different experimental groups, to document skeletal muscle and heart tissue lesions at baseline (referred to as "DMD pathological status").

Table 1. Distribution of animals in all experimental groups

Age at injection	Genotype	Experimental group	Number	Time of sacrifice (p.i.)
2 months	WT	vehicle	5	3 months
			7	6 months
	DMD*^mdx^*	vehicle	6	3 months
			4	6 months
		1×10^{13} vg/kg	5	3 months
			6	6 months
		3×10^{13} vg/kg	6	3 months
			5	6 months
		1×10^{14} vg/kg	5	3 months
			6	6 months
		3×10^{14} vg/kg	5	3 months
			5	6 months
		baseline pathological status	5	0 months
Older rats				
4 months	WT	vehicle	6	3 months
	DMD*^mdx^*	1×10^{14} vg/kg	6	3 months
		vehicle	6	3 months
		baseline pathological status	6	0 months
6 months	WT	vehicle	6	3 months
	DMD*^mdx^*	1×10^{14} vg/kg	6	3 months
		vehicle	6	3 months
		baseline pathological status	6	0 months

DMD*^mdx^*, Duchenne muscular dystrophy rat model; Vehicle, phosphate buffered saline 1X, 350 mM sodium chloride and 5% sorbitol +1.25% human serum albumin; p.i., post injection.

Vector biodistribution in DMD*^mdx^* rats treated with fordadistrogene movaparvovec

Body-wide AAV9 vector biodistribution

Using a quantitative PCR (qPCR) assay with a probe specific for the mini-dystrophin sequence, vector biodistribution was assessed in samples obtained at sacrifice. No qPCR signal was detected in whole blood at euthanasia (data not shown), confirming that vector genome detection was restricted to the non-blood tissues analyzed. The mean transgene copy numbers obtained in each tissue for each experimental group were plotted as vector genomes per diploid genome (vg/dg) in Figures 1A and 1B. Transgene DNA was detected in biceps femoris, pectoralis, spleen, liver, diaphragm, and heart samples in all vector-injected animals regardless of age at the time of injection (2, 4, or 6 months) or the time of sacrifice (3 or 6 months p.i.). The highest copy numbers were detected in the liver (as expected for AAV9), with levels that were ~10- to 45-fold higher than in the heart and ~40- to 300-fold higher than in the skeletal muscle. The lowest copy numbers were in the spleen.
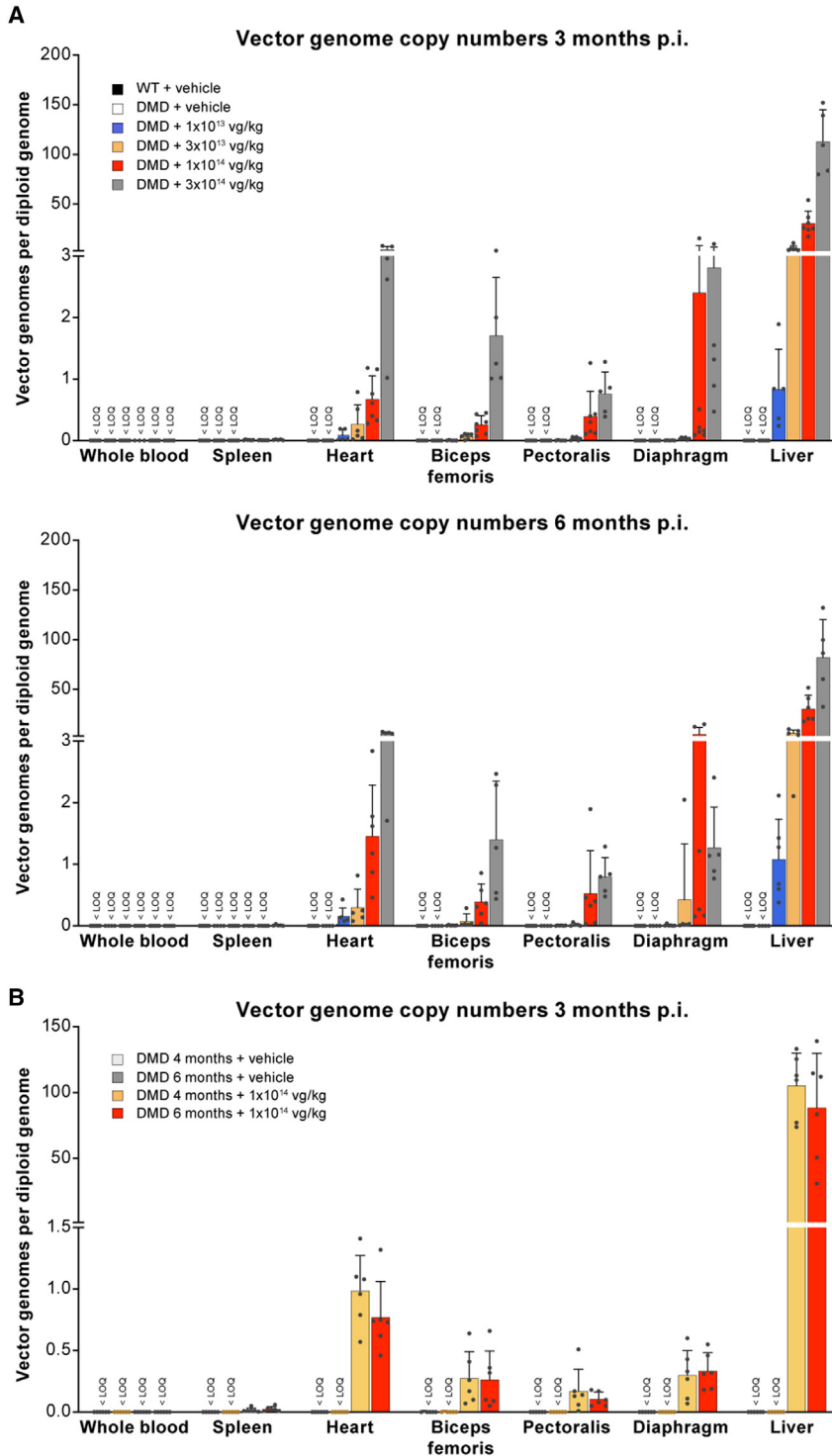
A

imals treated with the 1×10^{14} vg/kg dose and ∼5 vg/dg with 3×10^{14} vg/kg (5-fold increase). At 1×10^{14} vg/kg, transgene copy numbers in biceps femoris and pectoralis muscles were similar but did not reach levels above ∼0.5 vg/dg. When the dose was increased to 3×10^{14} vg/kg, the transgene copy number increased to ∼1.2 vg/dg (2-fold increase). The transduction efficiency of the diaphragm was more heterogeneous between animals, especially at the 1×10^{14} vg/kg dose, but transgene copy numbers reached a maximum of ∼3–4 vg/dg at the 1×10^{14} vg/kg or 3×10^{14} vg/kg dose (Figure 1A). The mean transgene copy numbers obtained in each tissue for each experimental group in older rats are shown in Figure 1B. The pattern of transgene copy distribution in tissues largely mirrored that in the dose-range study, with total copy numbers largely similar between animals injected with the 1×10^{14} vg/kg dose at 4 and 6 months of age.

Skeletal and cardiac muscle expression of mini-dystrophin protein following systemic administration of fordadistrogene movaparvovec

At 3- and 6-month follow-ups in the dose-range study, a dose-dependent increase in the percentage of mini-dystrophin-positive fibers was observed in all muscles evaluated (biceps femoris, heart, and diaphragm) following injection of the vector in 2-months-old DMD^{mdx} rats in the dose-range study. The expression observed was similar in its subsarcolemmal localization for all doses of vector administered (Figures 2A, 3A, and S1A). Compared with DMD^{mdx} control rats, an increase in the percentage of mini-dystrophin-positive fibers was observed in the biceps femoris, heart, and diaphragm for all doses tested at both time points. These differences reached statistical significance in the biceps femoris at 1×10^{14} vg/kg or greater at 3 months p.i., in the heart at 3×10^{14} vg/kg at both time points, and in the diaphragm at 1×10^{14} vg/kg or

At 3 and 6 months p.i., vector copy numbers in the liver reached a mean of ∼30 vg/dg in animals treated with the 1×10^{14} vg/kg dose and ∼80–110 vg/dg with 3×10^{14} vg/kg (∼3-fold increase over the starting dose). In the heart, levels reached a mean of ∼1 vg/dg in an-

A Biceps femoris muscle DYS – WGA

B

C Biceps femoris muscle DYS – WGA – DAPI

D
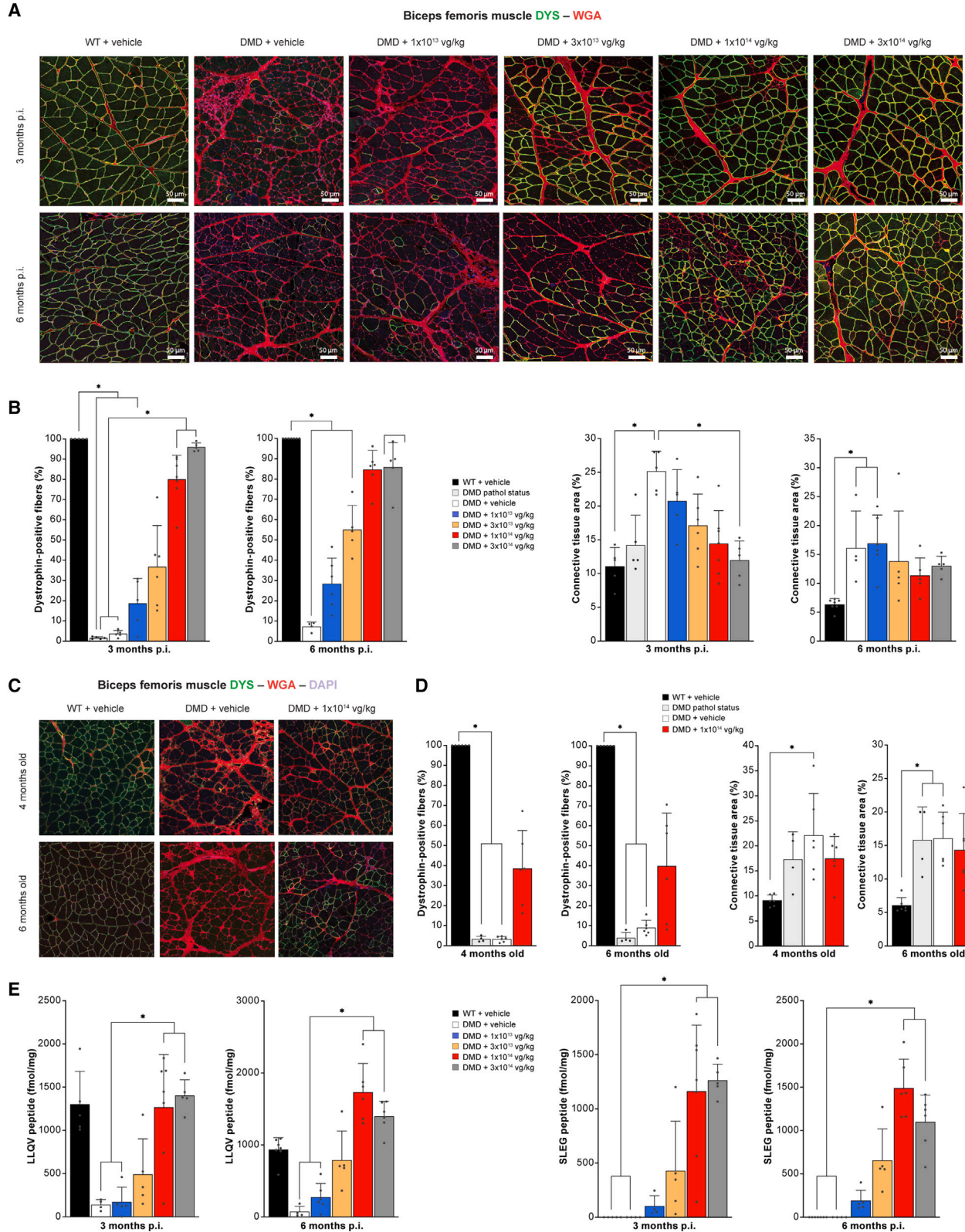
E

greater at 3 months p.i. and at 3×10^{14} vg/kg at 6 months p.i. (Figures 2B, 3B, and S1B). At the highest dose tested, the percentage of mini-dystrophin-positive fibers in DMD^{mdx} rats approached WT control values, with a mean of 80%–90% of mini-dystrophin-positive fibers in the biceps femoris and heart and 65%–75% of mini-dystrophin-positive fibers in the diaphragm. Sustained expression was observed, as shown by similar percentages of mini-dystrophin-positive fibers at 6 months p.i. compared with 3 months p.i. (Figures 2B, 3B, and S1B).

Administration of 1×10^{14} vg/kg of vector to older (4- and 6-month-old) DMD^{mdx} rats also resulted in an increase in the percentage of mini-dystrophin-positive fibers in the biceps femoris, heart, and diaphragm compared with age-matched DMD^{mdx} control rats 3 months p.i. (Figures 2C, 2D, 3C, 3D, S1C, and S1D). Interestingly, at 3 months p.i., the increase in the percentage of mini-dystrophin-positive fibers was greater in the biceps femoris in the DMD^{mdx} rats treated at 2 months of age ($\sim$80%; Figure 2B) compared with that seen in the biceps femoris of rats treated at 4 or 6 months of age ($\sim$40%; Figure 2D), whereas there was no significant effect of age on the percentage of positive fibers in the heart ($\sim$50%; Figures 3B and 3C) or diaphragm ($\sim$40%; Figures S1B and S1C).

Correlating with these data, mini-dystrophin protein was analyzed by western blot for 2 animals in each experimental group. Representative data are presented in Figures S2A and S2B. Mini-dystrophin of 153 kDa was detected in the biceps femoris, heart, and diaphragm of these DMD^{mdx} rats injected with the vector at doses of 3×10^{13}, 1×10^{14}, or 3×10^{14} vg/kg. In DMD^{mdx} rats injected with 1×10^{13} vg/kg, the mini-dystrophin protein was detected in the heart, biceps femoris, and, to a lesser extent, in the diaphragm (Figures S2A and S2B). Consistent with use of a muscle-specific promoter (human creatine kinase [hCK]), no mini-dystrophin protein was detected by western blot in the livers of DMD^{mdx} rats treated with all doses of the vector (Figures S3A and S3B). In older rats, relatively high levels of expression of mini-dystrophin protein were detected in biceps femoris, heart, and diaphragm samples from all DMD^{mdx} rats that were treated with the 1×10^{14} vg/kg vector dose (Figure S2C). No mini-dystrophin protein was detected in the liver of vector-treated older DMD^{mdx} rats (Figure S3C).

Finally, mini-dystrophin protein levels were quantified in the biceps femoris muscles at 3 and 6 months p.i. of the vector in 2-month-old DMD^{mdx} rats in the dose-range study using the recently described peptide immunoaffinity liquid chromatography-tandem mass spectrometry (IA-LC-MS/MS).[38] Mini-dystrophin protein expression was measured using two peptides, LLQV (present in the endogenous dystrophin and in the mini-dystrophin protein) and SLEG (present only in the mini-dystrophin protein). Compared with DMD^{mdx} control rats, an increase in mini-dystrophin expression levels was observed for all doses tested at both time points. These differences reached statistical significance at 1×10^{14} vg/kg or greater at 3 months p.i. (Figure 2E). Expression of both peptides (LLQV and SLEG) was comparable. At the highest dose tested, the levels of mini-dystrophin protein expression in DMD^{mdx} rats approached WT control values, and sustained expression was observed at 6 months p.i. compared with 3 months p.i. (Figure 2E).

Fordadistrogene movaparvovec reduces muscle lesions and fibrosis in DMD^{mdx} rats

DMD^{mdx} rats display skeletal and cardiac muscle necrosis, regeneration, and fibrosis, which are lesions typically seen in patients with DMD.[34] Analysis of muscle samples from all DMD^{mdx} rats revealed myopathic lesions typical of this rat model: presence of regenerative activity, as evidenced by centro-nucleated fibers and small foci of regeneration; presence of degenerated fibers, isolated or in small clusters; tissue remodeling; and fiber replacement by fibrotic or adipose tissue. The severity of these lesions varied considerably between rats and muscle types. Given this variability, skeletal and cardiac muscle lesions were semi-quantitatively scored on a scale of 0 (no lesion) to 3 (severe lesions), as illustrated in Figure S4. A mean individual score was then calculated based on the scores obtained for the biceps femoris, pectoralis, diaphragm, and cardiac muscle. We chose to perform this semi-quantitative analysis to provide a more global evaluation of the whole dystrophic lesion (i.e., presence of some regenerative activity, as evidenced by centro-nucleated fibers and small regenerative foci; presence of degenerated fibers; tissue remodeling; and fiber replacement with fibrotic or adipose tissue). The data showed a dose-responsive improvement of this histopathologic score (Figure 4A) at 3 months and 6 months p.i. and regardless of the injected dose. In older rats dosed with 1×10^{14} vg/kg at 4 and 6 months,

Figure 2. Immunohistochemical analysis of mini-dystrophin expression and assessment of fibrosis in the biceps femoris muscle
(A) Representative images of biceps femoris muscle sections collected 3 and 6 months p.i. from the following groups of rats 2 months old at the time of injection: WT+vehicle, DMD^{mdx} pathol status, DMD^{mdx}+vehicle and vector-injected DMD^{mdx} rats. The NCL-DYSB antibody was used to detect dystrophin/mini-dystrophin expression (green), and Alexa Fluor 555 WGA conjugate was used to detect connective tissue (red). DRAQ5 fluorescent DNA dye was used to detect nuclei. (B) Quantification of dystrophin and fibrosis labeling in sections from 2-month-old treated rats (samples collected at 3 or 6 months p.i.). Left panel: percentage of dystrophin-positive fibers. Right panel: percent area occupied by WGA-labeled connective tissue. (C) Representative images of biceps femoris muscle sections collected 3 months p.i. from the following groups of rats 4 and 6 months old at the time of injection (samples collected at 3 months p.i.): WT+vehicle-, DMD^{mdx}+vehicle-, and vector-injected DMD^{mdx} rats. The NCL-DYSB antibody was used to detect dystrophin/mini-dystrophin expression (green), and Alexa Fluor 555 WGA conjugate was used to detect connective tissue (red). DRAQ5 fluorescent DNA dye was used to detect nuclei. (D) Quantification of dystrophin and fibrosis labeling in sections from 4- to 6-month-old treated rats (samples collected at 3 months p.i.). Left panel: percentage of dystrophin-positive fibers (mean ± SD). Right panel: percent area occupied by connective tissue as labeled by WGA (mean ± SD). (E) IA-LC-MS/MS-based quantification of dystrophin/mini-dystrophin expression levels in biceps femoris samples from 2-month-old treated rats (samples collected at 3 or 6 months p.i.). Left panel: total dystrophin expression levels based on peptide LLQV. Right panel: mini-dystrophin expression levels based on peptide SLEG. Results are expressed as the mean ± SEM. *p < 0.05 (nonparametric Kruskal-Wallis test followed by a post hoc Dunn's multiple-comparisons test). WGA, wheat germ agglutinin; WT, wild-type; pathol, pathological.
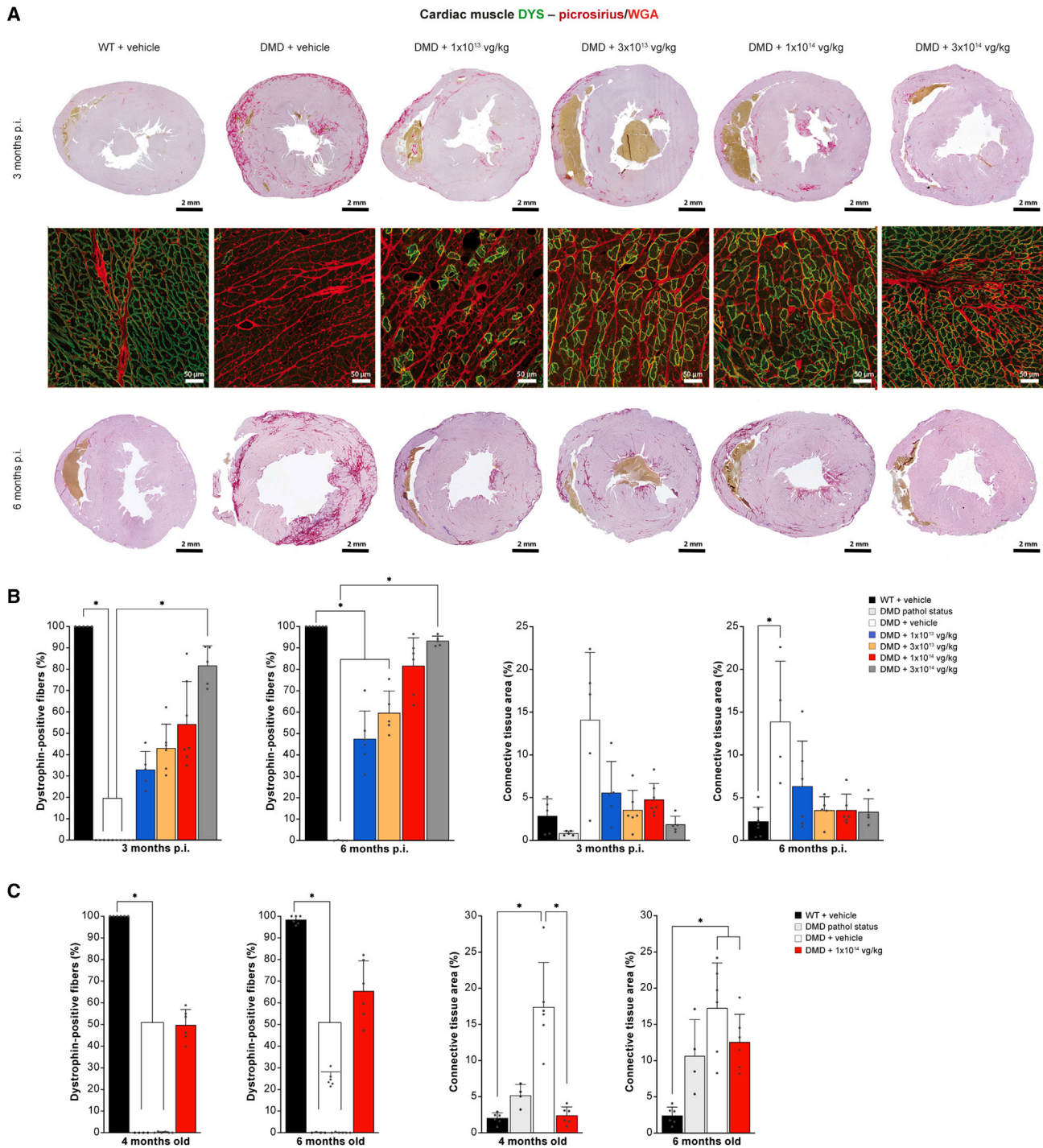
Figure 3. Immunohistochemical analysis of mini-dystrophin expression and assessment of fibrosis in the heart

(A) Transverse sections done at the level of the apex were stained NCL-DYSB antibody to detect dystrophin/mini-dystrophin expression (green), with picrosirius red for connective tissue (purple) and WGA conjugate (red) for connective tissue. Representative images correspond to samples collected 3 and 6 months p.i., from WT+vehicle, DMD^{mdx}+vehicle, and vector-injected DMD^{mdx} rats. (B) Quantification of dystrophin and fibrosis labeling in sections from 2-month-old treated rats (samples collected at 3 or 6 months p.i.). Left panel: percentage of dystrophin-positive fibers. Right panel: percent area occupied by picrosirius red-positive connective tissue. (C) Quantification of dystrophin and fibrosis labeling in sections from 4- and 6-month-old treated rats (samples collected 3 months p.i.). Left panel: percentage of dystrophin-positive fibers. Right panel: percent area occupied by picrosirius red-positive connective tissue. Results are expressed as the mean ± SEM. *p < 0.05 (nonparametric Kruskal-Wallis test, followed by a post hoc Dunn's multiple-comparisons test).
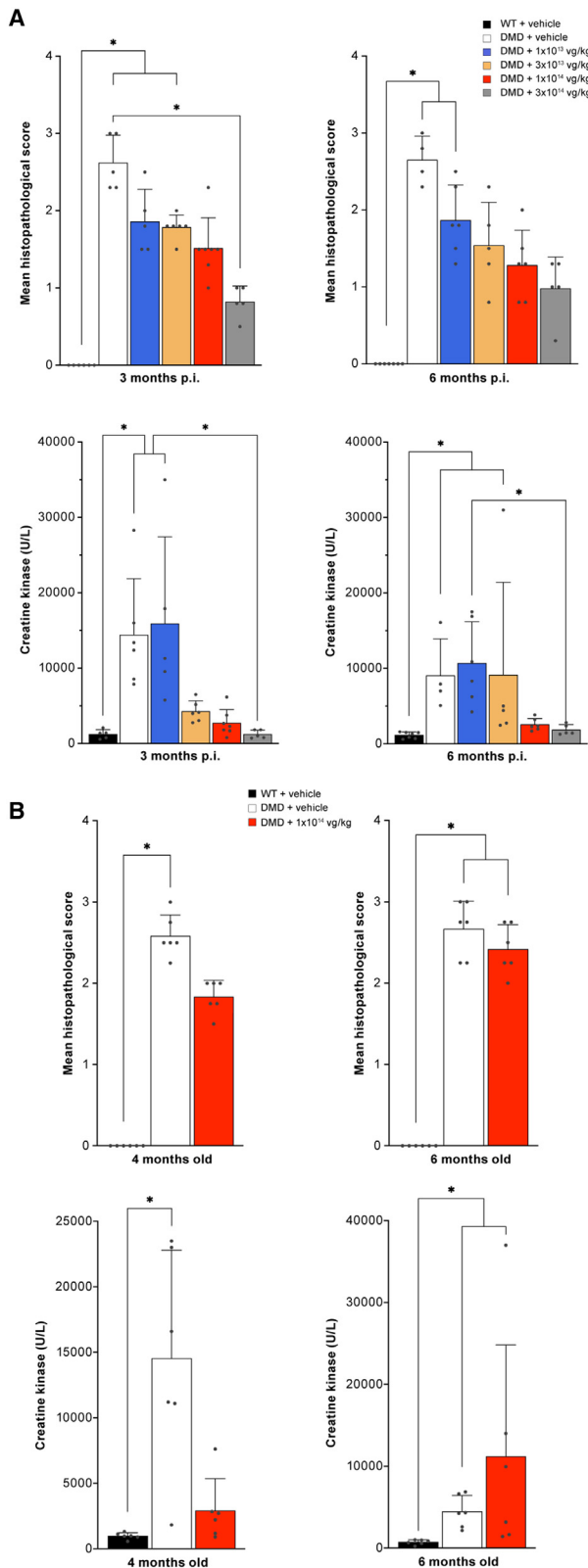
Figure 4. Muscle histopathology and serum CK levels

(A) Muscle histopathological score obtained after histopathological observation of muscle samples obtained at 3 and 6 months p.i. in rats injected at 2 months of age and serum CK levels (U/L) obtained in the same animals. (B) Muscle histopathological score obtained after histopathological observation of muscle samples obtained at 3 months p.i. in rats injected at 4 and 6 months of age and serum CK levels (U/L) obtained in the same animals. Results are expressed as the mean ± SEM. *p < 0.05 (nonparametric Kruskal-Wallis test followed by a post hoc Dunn's multiple-comparisons test).

after 3 months, the mean histopathologic score was also reduced compared with the untreated DMD^{mdx} controls. However, the magnitude of the reduction was smaller in the older rats dosed at 6 months of age (Figure 4B).

In the dose-range study, a qualitative assessment of regenerating fibers in vector-treated DMD^{mdx} rat biceps femoris sections also suggested a reduction of fiber regeneration (fewer developmental myosin heavy-chain-positive areas) with an observed dose-responsive reduction (Figure S5).

The percentage of surface occupied by connective tissue (marker of fibrosis) was measured in 3 randomly selected microscopic fields from biceps femoris and diaphragm sections after labeling muscle sections with a fluorescent wheat germ agglutinin (WGA)-conjugated probe[39] and from the heart after staining with picrosirius red. In the DMD baseline pathologic status group sacrificed at 2 months of age, the percentage areas of connective tissue in the biceps femoris muscle and in the heart were not significantly different from that observed in the WT control rats, suggesting very limited fibrosis at this age in DMD^{mdx} rats (Figures 2B and 3B). However, fibrosis was already evident in diaphragm sections collected at 2 months of age (Figure S1B). In the DMD^{mdx} control rats (at 5 and 8 months old), fibrosis had progressed and was significantly increased compared with the WT control group in the biceps femoris, the heart, and the diaphragm. In the dose-range study, treatment with vector resulted in a reduction in fibrosis. Indeed, compared with DMD^{mdx} control groups, reductions in fibrosis were observed at 3 months p.i. in the biceps femoris and in the heart from DMD^{mdx} rats treated with vector doses starting at the lowest dose tested (1×10^{13} vg/kg), with statistical significance reached in the biceps femoris at 3×10^{14} vg/kg. Importantly, for doses of 3×10^{13} vg/kg or greater in the biceps femoris and for doses of 1×10^{13} vg/kg or greater in the heart, the levels of fibrosis were very close to those observed in WT rats and in the DMD baseline pathologic status group, indicating that, at these doses, fordadistrogene movaparvovec prevented fibrosis in the heart and biceps femoris (Figures 2B and 3B). However, at 3 months p.i., no clear reduction of fibrosis was observed in the diaphragm regardless of the injected dose.

At 6 months p.i., a clear reduction in fibrosis was still observed in the heart at all doses and in the biceps femoris from the 3×10^{13} vg/kg dose group compared with the DMD^{mdx} control group, and a reduction was also observed in the diaphragm of DMD^{mdx} rats that received 3×10^{14} vg/kg (Figures 2B, 3B, and S1B).

In the 4- and 6-month-old DMD^{mdx} rats, marked fibrosis was already evident in the biceps femoris, heart, and diaphragm (>15%, >5%, and >35% fibrotic area, respectively), with no further increase observed 3 months later (compared with the DMD^{mdx} baseline pathologic status and the DMD^{mdx} and vehicle groups). Vector treatment had no effect on this established fibrosis 3 months p.i. in biceps femoris and diaphragm (Figures 2D and S1C). In the heart, a significant reduction of fibrosis levels was seen in the animals treated at 4 months of age but not in the animals treated at 6 months of age (Figure 3C).

Fordadistrogene movaparvovec improved body weight and circulating biomarkers in DMD^{mdx} rats

No adverse effects were observed with the injection procedure, and no morbidity or mortality could be attributed to the vector. Also, treatment with the vector had no negative impact on hematologic parameters (red blood cells count, hemoglobin, hematocrit, mean corpuscular volume, mean corpuscular hemoglobin, mean corpuscular hemoglobin concentration, reticulocytes, white blood cells, neutrophils, lymphocytes, monocytes, eosinophils, basophils, and platelets) or clinical biochemical parameters (urea, creatine, alkaline phosphatase, aspartate aminotransferase [AST], alanine aminotransferase [ALT], and lactate dehydrogenase [LDH] total serum proteins, and total bilirubin) that were evaluated at 3 and 6 months p.i. (data not shown). Weekly body weight assessments revealed that vector treatment had no negative impact on increasing body weight associated with animal growth (DMD^{mdx} rats dosed at 2 months of age). Although there was variability between animals within the different groups, increased body weight was observed at each time point examined compared with DMD^{mdx} control rats, with a dose-response effect (non-statistically significant) observed after 12 weeks p.i. (Figure S6A). In the DMD^{mdx} rats that were injected with 1×10^{14} vg/kg vector at older ages, growth-associated body weight increases were also observed few weeks after vector treatment. This was particularly evident in the rats injected at 6 months of age, whose body weights did not increase over the time course of the study in the control group but in which vector treatment induced a body weight increase across the course of the study (Figures S6B and S6C).

In patients with DMD, muscle damage is characterized by an increase of creatine kinase (CK) activity in the blood. In DMD^{mdx} control rats in the dose-range study, serum CK levels were significantly higher compared with those in WT control rats at similar ages (5 and 8 months old) (Figure 4A). Treatment with the 2 highest doses of vector (1×10^{14} and 3×10^{14} vg/kg) resulted in a 75%–90% reduction in serum CK levels at 3 and 6 months p.i.; this reduction was statistically significant in the 3×10^{14} vg/kg dose group and reached CK levels comparable with the WT controls rats at both time points. A reduction in CK levels was also observed in the 3×10^{13} vg/kg dose group at 3 months p.i., which did not reach statistical significance (compared with DMD^{mdx} control rats). The lowest dose of vector tested (1×10^{13} vg/kg) had no effect on CK levels at either time point (Figure 4A). In the older cohorts of DMD^{mdx} rats, mean serum CK levels were significantly higher in DMD^{mdx} control versus WT control rats (at 7 and 9 months of age) (Figure 4B). Interestingly, CK levels were lower in

the 9-month-old DMD^{mdx} rats compared with the 5- and 7-month-old rats, reflecting the reduced muscle function and muscle loss in older rats, which has also been reported in patients with DMD.[40] In animals injected at 4 months of age, mean CK levels at sacrifice were lower in vector-treated animals than in DMD^{mdx} control animals, although this difference was not significant. Interestingly, in the DMD^{mdx} rats treated at 6 months of age, CK levels were increased compared with the DMD^{mdx} control group, although this was not statistically significant (Figure 4B).

AST, ALT, and LDH are known biomarkers of DMD that are released from damaged skeletal muscle and heart during the active phase of the disease. In DMD^{mdx} control rats, the level of all these biomarkers is increased compared with WT control rats regardless of age (Figures S7A–S7C). AST levels were reduced only in the 3×10^{14} vg/kg groups at 3 and 6 months p.i. In the lower-vector-dose groups (regardless of the age at injection), AST levels were not significantly different from the DMD^{mdx} control rats (Figures S7A and S7B).

For ALT and LDH, treatment with vector induced a dose-dependent decrease in these biomarker levels 3 months p.i., reaching, with the 1×10^{14} and 3×10^{14} vg/kg doses of vector, levels that were similar to those of WT control rats (Figures S7C and S7E). Because ALT and LDH levels were not significantly increased in the 8-month-old DMD^{mdx} rats compared with age-matched WT rats, no clear conclusions about the effect of vector treatment 6 months p.i. can be made (Figures S7C and S7E). In older rats, ALT and LDH levels were decreased after vector treatment in 4-month-old DMD^{mdx} rats only. No effect was observed in the DMD^{mdx} rats treated at 6 months of age (Figures S7D and S7F).

Expression of mini-dystrophin in skeletal and cardiac muscle improves their function
Improvements in skeletal muscle function

As reported previously,[34] DMD^{mdx} rats exhibit reduced muscle strength and increased fatigue compared with WT controls. The effect of vector treatment on muscle fatigue was assessed by quantifying grip force in rats across 5 successive grip strength testing trials, with a short interval between each trial. A reduction in grip force between the first and last trial represents an index of fatigue. Compared with WT control rats and at all ages examined, the DMD^{mdx} control rats exhibited a progressive and significant decrease in grip strength at each of the 5 trials at all times that were evaluated (5, 7, 8, or 9 months old) (Figure 5). Vector treatment induced a dose-dependent preservation of grip force observed during repeat grip force trials in DMD^{mdx} rats at 3 and 6 months p.i. (Figures 5A and 5B). This became evident in the rats dosed with 3×10^{13} vg/kg or greater of vector (no benefit was observed at the lowest dose tested, 1×10^{13} vg/kg). At 3×10^{13} vg/kg at 3 months p.i., preservation of grip force was observed until trial 3, with a grip force statistically greater than that of DMD^{mdx} control rats and similar to that of WT control rats. Also, at the end of trial 5, the grip force decline in this dose group was less pronounced compared with the DMD^{mdx} control rats (33% ± 7% reduction in grip force with 3×10^{13} vg/kg vector compared with 63% ± 5% reduction in
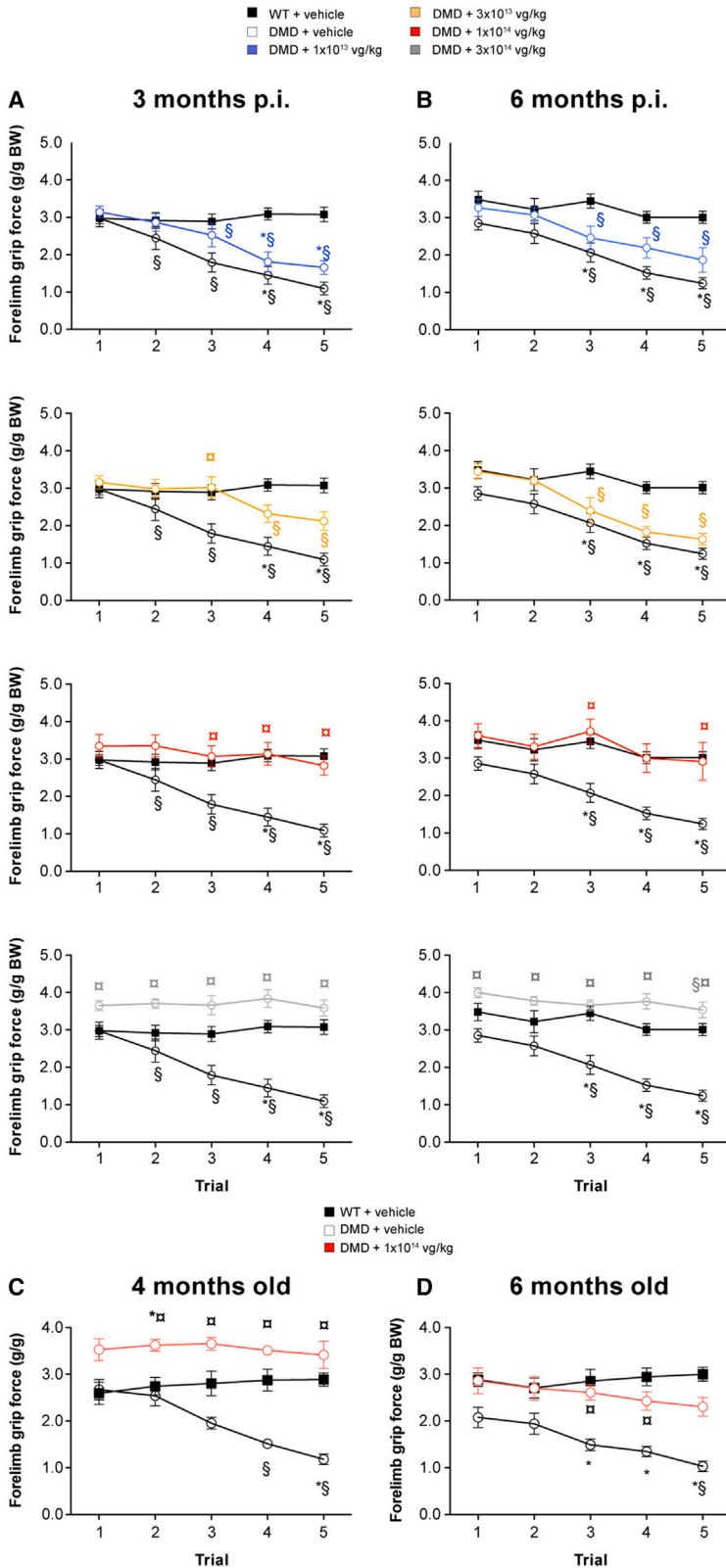
Figure 5. Assessment of mini-dystrophin expression on skeletal muscle function

(A and B) Dose-range study of vector injected in DMD^{mdx} rats at 2 months of age and evaluated in grip strength assessments over 5 successive trials (grip strength tests) at 3 (A) and 6 (B) months p.i. Data plots show the mean forelimb grip force (g/g normalized to body weight [BW]) ± SEM collected at each trial for each dose of vector. (C) Evaluation of muscle function in DMD^{mdx} rats injected with 1×10^{14} vg/kg vector at 4 and 6 months of age (grip strength tests, as described above). Data represent the mean forelimb grip force (g/g normalized to BW) ± SEM collected at each trial 3 months p.i. Left panel: rats dosed at 4 months of age. Right panel: rats dosed at 6 months of age. *p < 0.05 vs. WT. ¤p < 0.05 vs. DMD^{mdx} control rats. §p < 0.05 vs. trial 1 (non-parametric Friedman test followed by Dunn's post hoc test).

DMD^{mdx} control rats; Figure S8A). At 6 months p.i. with 3×10^{13} vg/kg vector, no preservation of grip force was observed. However, at 1×10^{14} and 3×10^{14} vg/kg vector, complete preservation of grip force at each of the 5 trials was observed at 3 and 6 months p.i. (Figures 5B and S8B). Even in the older DMD^{mdx} rats dosed with 1×10^{14} vg/kg at 4 months of age, no decline in grip force was observed over the course of the trials (Figures 5C and S8C). In the rats dosed at 6 months of age (9 months old at the time of the grip force trials) with 1×10^{14} vg/kg, grip force was higher than that observed in the DMD^{mdx} control rats, with a significant difference between the 2 groups at trials 3 and 4 (Figure 5D). However, there was a progressive decrease in grip force over the course of the trials in the oldest rats, with an overall decrease of 16% ± 9% between trial 1 and trial 5 (Figure S8D).

When examining the maximal muscle grip strength at the end of the study, a reduction in absolute maximum grip force was observed between WT and DMD^{mdx} control animals regardless of the age of the animals (Figure S8). When grip force was normalized to body weight (relative maximum grip force), the reduction of grip force was still observed, with statistical significance reached in the oldest (9-month-old) rats (Figure S8). Vector treatment of 2-month-old DMD^{mdx} rats resulted in a dose-dependent increase in absolute and relative maximum grip force 3 and 6 months p.i. Compared with untreated DMD^{mdx} rats, the increased force was statistically significant in the rats that received 1×10^{14} and 3×10^{14} vg/kg at 3 months p.i. and in the rats that received 3×10^{14} vg/kg at 6 months p.i. (Figures S8A and S8B). Vector treatment of the older DMD^{mdx} rats (1×10^{14} vg/kg at 4 and 6 months of age) also resulted in an increase in absolute and relative grip force (Figures S8C and S8D).

Improvements in cardiac remodeling and function
Cardiac function was assessed in all rats using 2D echocardiography and Doppler analysis. The parameters looking at structural remodeling (i.e., free-wall diastolic thickness and left ventricle [LV] end-diastolic diameter of the DMD^{mdx} rat hearts) evolved with time. At ∼3 months of age, LV hypertrophy is common in DMD^{mdx} rats.[34] The transition to measurable ventricle dilatation seen in older rats (>8–9 months old) is characterized by the absence of noticeable wall thickness or abnormal ventricle diameter. This transition phase occurs around 5–7 months of age.[41] Therefore, at 3 months p.i. in the dose-range study (i.e., at 5 months of age), no structural remodeling was observed in the DMD^{mdx} control rats. As a consequence, there was no apparent difference between treated and untreated rats evaluated at 5 months of age (Figure 6A). However, compared with age-matched WT control rats at 6 months p.i. (DMD^{mdx} rats ∼8 months old) and at 7–9 months of age (3 months p.i.) in the older rats, the DMD^{mdx} control rats exhibited an increasing trend in LV end-diastolic diameter that was prevented at all vector doses (Figure 6A). Cardiac function was evaluated by measuring systolic (LV ejection fraction [LVEF]; Figure S9A) and diastolic parameters (early/late diastolic [E/A] velocity ratio [Figure 6B], isovolumetric relaxation time [IVRT; Figure 6C], and deceleration time [DT; Figure S9B]). Of note, because of experimental difficulties, DT was not measured in 5-month-old animals.

When comparing WT and DMD^{mdx} control rats, the diastolic function was found to be disturbed regardless of the age of the animals (Figures 6B, 6C, and S9B). In the dose-range study at 3 months p.i., E/A ratio and IVRT value were partially restored in the treated animals without any clear dose effect (Figures 6B and 6C). At 6 months p.i., E/A ratios were also only partially restored, but IVRT and DT values appeared to be fully restored without any dose effect and reached mean values that did not significantly differ from those of WT control rats (Figures 6B, 6C, and S9B). Finally, in the older rats, injection of 1×10^{14} vg/kg at 4 or 6 months of age induced complete correction of the diastolic dysfunction with improved E/A ratios as well as IVRT and DT values (Figures 6B, 6C, and S9B).

In line with the lack of structural remodeling in 5-month-old animals of the dose-range study (at 3 months p.i.), no difference in LVEF was observed between the control and experimental groups (Figure S9A). At 6-months p.i., despite the small number of animals in this group and the widespread values, a decreasing trend was seen in the DMD^{mdx} control rats compared with WT control rats (Figure S9A). The lowest LVEF value was observed in the animal displaying the most severe dilatation, supporting the relevance of our findings. Overall, LVEF values recorded in vector-treated DMD^{mdx} rats were similar to those of WT control rats (Figure S9A). These observations may indicate a corrective effect of the vector on systolic remodeling regardless of the dose administered. In 7- and 9-month-old DMD^{mdx} control rats, LVEF values were lower than in WT control rats, whereas vector-treated rats had similar LVEF values as WT control rats (Figure S9A). This suggests a corrective effect of the vector on systolic remodeling regardless of the age at which it is administered.

Evaluation of immune responses
Humoral and cellular immune responses to the transgene product and AAV9 capsid were monitored in serum samples and splenocytes obtained at 3 and 6 months p.i. No humoral or cellular immune response was detected in WT and DMD^{mdx} control rats.

Immunoglobulin G (IgG) antibody humoral response to the transgene product (mini-dystrophin) was analyzed by western blot (see Figure S10A for a representative result). A response to mini-dystrophin protein was observed in many of the vector-treated DMD^{mdx} animals (83%, 86%, and 100% of the rats at 2, 4, and 6 months of age), with no anti-transgene cellular immunity (interferon -γ [IFN-γ] secretion; see Figure S10B for a representative result) detected in any animal (Table S1).

Finally, a classic humoral response to the AAV9 capsid (IgG antibodies and neutralizing factors) was observed in all DMD^{mdx} rats exposed to the vector (data not shown). Also, a positive anti-capsid response (IFN-γ ELISpot assay) was observed in 37%, 67%, and 18% of DMD^{mdx} rats injected with vector at 2, 4, or 6 months of age, respectively (Table S2). Of note, a dose-dependent effect was observed, particularly between the 1×10^{13} vg/kg and 1×10^{14} vg/kg doses, similar to previously described dose effects observed in clinical trials of AAV-mediated gene therapy.[42,43]
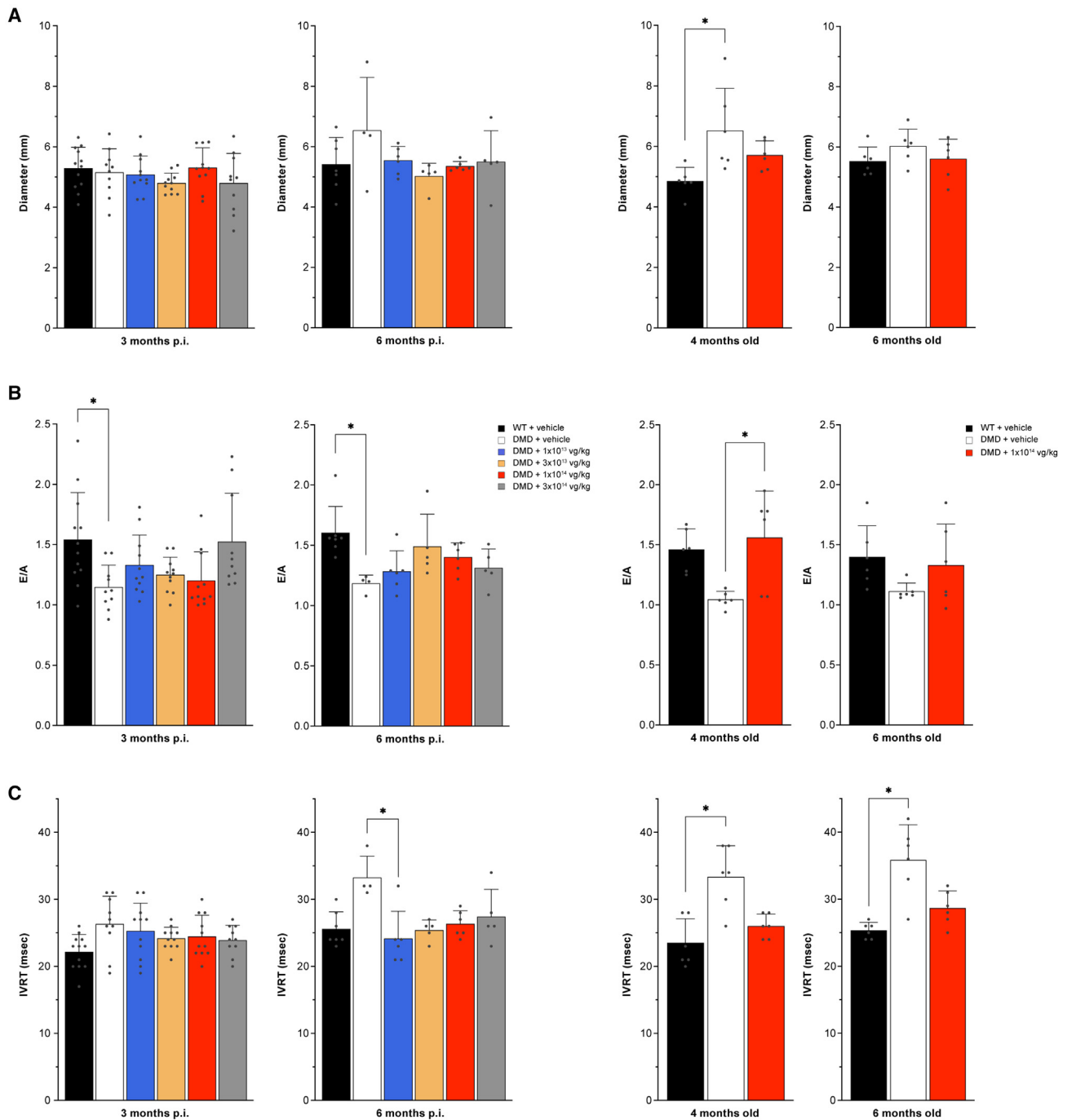
Figure 6. Assessment of mini-dystrophin expression on cardiac muscle function

(A) LV diastolic diameter measured during diastole from long-axis images obtained by M-mode echocardiogram. (B) E/A ratio measured using pulsed Doppler with an apical 4-chamber orientation. (C) IVRT measured using pulsed Doppler with apical 4-chamber orientation. Results are expressed as the mean ± SEM. *p < 0.05 (nonparametric Kruskal-Wallis test followed by a post-hoc Dunn's multiple-comparisons test). E/A, early/late diastolic velocity; IVRT, isovolumetric relaxation time; LV, left ventricle.

DISCUSSION

This is the first study that evaluated a candidate gene therapy, fordadistrogene movaparvovec, in development as a treatment for DMD, in a rat model of DMD. The candidate gene therapy comprises an rAAV9 vector for delivery of a codon-optimized human mini-dystrophin transgene to skeletal and cardiac muscle. The vector incorporates a

muscle-specific promoter to ensure expression of the transgene only in skeletal and cardiac muscle. A clinically relevant, well-tolerated dose was identified, which induced increased body weight, improved clinical chemistry parameters, and induced robust amelioration of skeletal and cardiac muscle histopathology as well as improvements in skeletal muscle and heart function. These changes correlated with tissue-specific expression of the mini-dystrophin protein. In older rats (4–6 months old), this well-tolerated efficacious dose of the vector also improved body weight and clinical chemistry parameters and induced skeletal and cardiac muscle expression of mini-dystrophin with measurable positive effects on skeletal and cardiac muscle function. These results therefore suggest that treatment with fordadistrogene movaparvovec may also provide clinical benefits in later stages of DMD.

In 2014, Larcher et al.[34] and Nakamura et al.[44] described the first rat models of DMD. It was thought that a rat model could represent a useful alternative to GRMD dogs because rats are small relative to dogs but 10 times larger than mice and, therefore, may better reflect the lesions and functional abnormalities observed in patients with DMD. It has been shown that the DMD^{mdx} rat model described by Larcher et al.[34] was more representative of patients with DMD in terms of the tissues affected (i.e., rapidly evolving cardiac and skeletal muscle pathology) and progression of severity with increased age.[36,45–47] The DMD^{mdx} rat model was used here to evaluate the efficacy of fordadistrogene movaparvovec. Moreover, we employed a state-of-the-art translational dose-finding study with randomization of animals, established standard operating procedures, a quality-controlled environment, and blinded analyses to identify the minimally effective dose (MED), which was then evaluated in older rats with a more dystrophic pathology. To mimic the planned clinical studies, a single intravenous administration of the vector was tested.[41] No immunosuppressant regimen was used in these studies to characterize the immune response to the transgene and capsid.

The relatively short duration of the study (DMD^{mdx} rats treated at 2 months of age and sacrificed after 3 or 6 months or older rats treated at 4 or 6 months of age and sacrificed after 3 months) was required because of the aggressive pathology in this animal model, leading to a life expectancy of approximately 1 year. Fibrosis is a major aspect of the dystrophic pathology in DMD^{mdx} rats; therefore, this was quantified as part of the histopathology in parallel with the quantification of the mini-dystrophin-positive fibers. A semi-quantitative evaluation of the dystrophic lesions was also conducted. No cellular immunity against dystrophin, even in the absence of immunosuppression, was observed in this study, whereas such responses have been observed in immunosuppressed patients. This indicates, like in other similar models (mouse and dog), that the DMD^{mdx} rat model is not relevant to evaluate such immune responses. As a community, we consistently see limitations because of the translational implications of immune responses in almost all animal models studied to date, highlighting the need to develop other models to study immunity. Even with these general limitations, we were able to obtain significant functional and dose-dependent data that are tracking with clinical observations.

Indeed, this is the first study to demonstrate the efficacy of fordadistrogene movaparvovec in a more robust model of DMD disease progression that recapitulates cardiac disease, a known phenotype responsible for up to 75% of all DMD deaths.[48]

In this study, transgene DNA was detected in all vector-injected animals regardless of the dose, age of injection, and time of sacrifice. In all animals, the liver was the most efficiently transduced tissue, with copy numbers that were ∼10- to 45-fold higher than in the heart and ∼40- to 300-fold higher than in skeletal muscle. In older animals, despite severe and extended lesions in skeletal striated muscle and myocardium (degenerated fibers, tissue remodeling and fiber replacement with fibrotic or adipose tissue, cellular infiltrate) at the time of vector administration (4 and 6 months of age), the transduction levels and profiles observed were quite similar to those of the rats administered vector at 2 months of age. High levels of transgene DNA were expected in the liver because of the systemic route of administration of the AAV9 vector. The consequences of biodistribution of transgene DNA throughout multiple tissue types are unknown. Successful efforts to de-target the liver have been reported,[49] but none based on the AAV9 capsid, the serotype of choice to efficiently target the muscle tissues affected in DMD, had been described at the time the development program began. Thus, to mitigate against potential negative effects of off-target transgene expression, a muscle-specific promotor was included in the construct. The success of this approach is reflected in the lack of mini-dystrophin expression protein detected in the liver. Moreover, and importantly, liver histopathology was performed during our study and did not show any liver lesions that could be attributed to the treatment (data not shown).

It should be noted that the AAV9 vector biodistribution and transduction observed in rodents may be different in humans. Previous studies have documented that systemic delivery of AAV9 in mice transduced the heart more efficiently than any other natural serotype.[50–52] However, this superior cardio-tropism of AAV9 was not reported in dogs.[53] This tropism/species disparity is not unique to AAV9 and has been observed with an AAV8 vector currently being used in clinical trials in patients with hemophilia. Nonclinical studies using doses of 10^{10} vg of AAV8 with a Factor IX (FIX) transgene reached supra-physiologic levels (>100% of the WT) of FIX expression in a mouse model, 46% of normal in non-human primates, but just detectable FIX expression levels in humans at 2-log higher doses. It should be noted that the transduction efficiency of fordadistrogene movaparvovec in specific muscle groups may vary when characterized in larger animal models and more specifically in humans. Regardless, although the overall transduction efficiency may vary between species, the overall outcome of widespread tissue transduction appears to be consistent between mouse, rat, and canine models.

This dose-range study with fordadistrogene movaparvovec showed a dose effect for most of the evaluated parameters except for cardiac function. Indeed, improvements in cardiac function were observed at all doses. This absence of a dose effect could be correlated with the fact that a reduction of fibrosis levels was observed in the cardiac

tissue regardless of the injected dose. On the contrary, in skeletal muscle, a dose effect was observed for fibrosis levels and for muscle strength. Finally, we identified 1×10^{14} vg/kg as the MED, based on skeletal and cardiac muscle function endpoints and mini-dystrophin expression levels at 3 months p.i. This expression was sustained in DMD^{mdx} rats 6 months p.i. This dose was also therapeutically effective when administered to older, more dystrophic DMD^{mdx} rats, suggesting that it may also be effective in patients at later stages of disease. However, there was a less effective rescue of muscle function in the oldest cohort of DMD^{mdx} rats (6 months old at the time of injection) compared with younger rats, with a progressive decrease in grip force over the course of the trials. We think that even if the muscular pattern of the tissue is improved by the treatment in older animals, tendon retractions may be present at 6 months of age and may not be corrected by the treatment. This suggests that, in patients with DMD, the benefits of this gene therapy may be more apparent in younger than older patients. Although it is tempting to speculate that younger, less diseased muscle may be transduced more efficiently than older DMD tissue, it remains to be seen whether different capsid-specific mechanisms of transduction are at play. If so, then this would support development of second-generation vectors to overcome potential barriers to transduction associated with higher percentages of fat and necrosis observed in older versus younger, healthier muscle tissue. However, it should be noted that the MED of 1×10^{14} vg/kg identified in the current study has translated well for patients with DMD,[54] further emphasizing the relevance of DMD^{mdx} rats as a model for the human disease.

Several serum biomarkers, including CK, ALT, and LDH, were modulated by the vector in these studies, which indicates their potential utility in clinical trials. Importantly, the vector was well-tolerated in all rats, with no evidence of toxicity. There was also no evidence of deleterious immune system responses to the vector in terms of therapeutic efficacy and safety even though humoral and cellular responses to the capsid and humoral response to the transgene were detected. Taken together, these data show evidence of efficacy and safety in an appropriate disease model.

In conclusion, our data provide evidence of the overall safety and therapeutic efficacy of fordadistrogene movaparvovec following systemic administration in a rat model of DMD, supporting its use in clinical trials in patients with DMD. Importantly, the preliminary clinical trial data obtained in patients with DMD treated with fordadistrogene movaparvovec[55] also provides evidence of accurate translation of the MED determined here in DMD^{mdx} rats.

MATERIALS AND METHODS
Vector design and production
The fordadistrogene movaparvovec vector contained a species-specific codon and mRNA sequence-optimized human mini-dystrophin cDNA (Hopti-Dys3978, as described previously[27]) that was placed under the control of a human creatine kinase (hCK) muscle-specific promoter and of a synthetic polyadenylation (spA) signal. The batch of vector was produced using the Pro10 cell line (Viralgen, San Sebastián,

Spain) and the triple plasmid transfection system. Briefly, the Pro10 cells were cultured in chemically defined, serum-free medium at 37°C using a 50 L WAVE bioreactor (GE Healthcare Bio-Sciences, Uppsala, Sweden). After the Pro10 cells reached an optimal cell density in the bioreactor, a 3-plasmid (Ad helper, rep2/cap9, and inverted terminal repeats (ITR)-hCK.Hopti-Dys3978.spA) transfection cocktail was added to the bioreactor to produce AAV9 packaging the hCK.Hopti-Dys3978.spA therapeutic genome cassette. Approximately 48 h post transfection, the Pro10 cells were processed according to Clément and Grieger.[56] The vector was formulated in phosphate-buffered saline 1X, 350 mM sodium chloride, and 5% sorbitol; sterile filtered; aliquoted; and frozen at–60°C or lower. Quality control tests were performed, including genome copy titer measured by qPCR, infectious titer measured by median tissue culture infectious dose ($TCID_{50}$) assay, empty:full capsid ratio, endotoxin, purity, and bioburden/sterility (Table S3).

Animals and vector delivery protocols
This study included a dose-range portion in 4 groups of DMD^{mdx} rats $\sim$7–9 weeks ($\sim$2 months) old and a study in older DMD^{mdx} rats 4 and 6 months old. Additional control groups of age-matched DMD^{mdx} rates and age-matched WT rats were injected with formulation buffer (vehicle) only (Table 1). Animals were randomized, and the operators conducting the injections were blinded. The same batch of vector was administered to all animals in the study. The vehicle contained phosphate-buffered saline 1X, 350 mM sodium chloride, and 5% sorbitol with 1.25% human serum albumin.

For the dose-range study, 4 vector-treated groups received 1×10^{13} vg/kg (vg per kg of body weight), 3×10^{13} vg/kg, 1×10^{14} vg/kg, or 3×10^{14} vg/kg. Rats in the dose-range study were sacrificed at 3 or 6 months p.i. (Table 1). For the age study, animals received a single intravenous injection of 1×10^{14} vg/kg of the vector and were sacrificed at 3 months p.i. (Table 1).

All DMD^{mdx} and WT rats were from the same genetic background (Sprague-Dawley). Healthy and DMD^{mdx} rats were derived from the same litters, and all rats were bred (using carrier females and WT males) and maintained at the Boisbonne Center (Nantes Atlantic National College of Veterinary Medicine, Nantes, France). All procedures were conducted in conformity with European rules for animal experimentation (French Ethical Committee APAFIS 736-2015060118144661 v2, date of approval November 2, 2015; APAFIS 5657-2016061409503973 v1, date of approval November 10, 2016), and all efforts were made to minimize suffering. All injections were performed intravenously through the dorsal penile vein. Before injection, the analgesic buprenorphine (Vetergesic, 0.04 mg/kg) was administered between 30 min and 6 h before anesthesia with etomidate (Hypnomidate, 16–32 mg/kg, intraperitoneally [i.p.]), administered in 2–4 injections separated by 3 min. Buffer or vector was administered in a single injection in anesthetized animals at a flow rate of $\sim$1 mL/min and a total volume of 3.0–6.4 mL per animal was administered depending on body weight (151–295 g for DMD^{mdx} rats and 185–318 g for WT rats). In the experimental and

control groups, the total volume injected was ~20 mL/kg (although vector dose varied in each experimental group, the total volume injected per kilogram remained constant).

Vector biodistribution analysis

Whole blood was collected from anesthetized rats just prior to sacrifice. Genomic DNA (gDNA) was extracted from ~600 μL of whole blood using the Gentra Puregene Kit (QIAGEN, Germantown, MD, USA), according to the manufacturer's instructions. Splenocytes were isolated from fresh spleens immediately after sacrifice and stored in liquid nitrogen. The gDNA was extracted from ~25 million splenocytes using the Gentra Puregene Kit according to manufacturer's instructions. Other tissue samples (biceps femoris, pectoralis, liver [central lobe], diaphragm, and heart [apical region]) were obtained just after sacrifice under conditions that minimized cross-contamination and avoided qPCR inhibition.[57] Samples were snap-frozen in liquid nitrogen and stored at −70°C or lower before DNA extraction. The gDNA was extracted using the Gentra Puregene Kit and TissueLyserII (both from QIAGEN) according to the manufacturer's instructions. qPCR analyses were conducted on a StepOne Plus real-time PCR system (Applied Biosystems, Thermo Fisher Scientific) using 50 ng of gDNA in duplicate. All reactions were performed in duplicate in a final volume of 20 μL containing template DNA, Premix Ex taq (Ozyme, Saint-Cyr-L'École, France), 0.3 μL of ROX reference dye (Ozyme), 0.2 μmol/L of each primer, and 0.1 μmol/L of TaqMan probe. Vector copy numbers were determined using the following primer/probe combination, designed to amplify a region of the Hopti-Dys3978 transgene:

Forward: 5′-CCAACAAAGTGCCCTACTACATC-3′

Reverse: 5′- GGTTGTGCTGGTCCAGGGCGT-3′

Probe: 5′-FAM-CCGAGCTGTATCAGAGCCTGGCC-TAMRA-3′

Endogenous gDNA copy numbers were determined using a primer/probe combination designed to amplify the rat *HPRT1* gene:

Forward: 5′- GCGAAAGTGGAAAAGCCAAGT-3′

Reverse: 5′-GCCACATCAACAGGACTCTTGTAG-3′

Probe: 5′- JOE- CAAAGCCTAAAAGACAGCGGCAAGTTGAAT-TAMRA-3′

For each sample, cycle threshold (Ct) values were compared with those obtained with different dilutions of linearized standard plasmids (containing either the Hoptidys-3978 expression cassette or the rat *HPRT1* gene). The absence of qPCR inhibition in the presence of gDNA (obtained from whole blood, splenocytes, skeletal muscle, heart, and liver) was determined by analyzing 50 ng of gDNA extracted from tissue samples from a control animal, spiked with different dilutions of standard plasmid. The results obtained by simplex qPCR (independent amplification of each sequence) versus duplex qPCR (amplification of the 2 sequences in the same reaction) were then compared. Both sequences were amplified with the same efficacy and specificity under the 2 conditions. Subsequent analyses were performed using duplex qPCR. Results are expressed as vg/dg. The limit of quantification of our test was 0.002 vg/dg.

Western blot analysis of total mini-dystrophin protein

Tissue samples (biceps femoris, liver [central lobe], diaphragm, and heart [apical region]) were obtained immediately after sacrifice under conditions that minimized cross-contamination. Samples were snap-frozen in liquid nitrogen and stored at −70°C or lower before protein extraction. Total protein was extracted from tissue samples using RIPA buffer containing protease inhibitor cocktail (Sigma-Aldrich, Merck, Darmstadt, Germany). Protein extracts (50 μg for biceps femoris, heart, and diaphragm and 100 μg for liver) were loaded onto a NuPAGE Novex 3%–8% Tris acetate gel (Thermo Fisher Scientific, Waltham, MA, USA) and analyzed using the NuPAGE Large Protein Blotting Kit according to the manufacturer's instructions, except for the final concentration of dithiothreitol (DTT; 200 mM, to reduce proteins before loading). Membranes were then blocked in 5% skimmed milk, 1% NP-40 (Sigma-Aldrich) in TBST (Tris-buffered saline/0.1% Tween 20) and hybridized with an anti-dystrophin antibody specific for exons 10 and 11 of the dystrophin protein (1:100, MANEX 1011C [a monoclonal antibody obtained from the Muscular Dystrophy Association (MDA) Monoclonal Antibody Resource]) and with a secondary anti-mouse IgG horseradish peroxidase (HRP)-conjugated antibody (1:2,000, Dako Alligent, Santa Clara, CA, USA). As a protein-loading control, the same membrane was also hybridized with an anti-rat α-tubulin antibody (1:10,000, Sigma) and with a secondary anti-mouse IgG HRP-conjugated antibody (1:2,000, Dako). Immunoblots were visualized using the enhanced chemiluminescence (ECL) analysis system (Thermo Fisher Scientific).

IA-LC-MS/MS quantification of dystrophin and mini-dystrophin expression levels

Biceps femoris samples were obtained immediately after sacrifice under conditions that minimized cross-contamination. Samples were snap-frozen in liquid nitrogen and stored at −70°C or lower before protein extraction. Tissue lysis, protein extraction, precipitation, digestion, and positive-pressure filtration were performed as described previously.[38] IA-LC-MS/MS quantification of dystrophin and of mini-dystrophin using the LLQVAVEDR (LLQV) and SLEGSDDAVLLQR (SLEG) peptides, specific of dystrophin/mini-dystrophin and of mini-dystrophin, respectively, was also performed as described previously.[38]

Immunolabeling of mini-dystrophin-positive fibers and histopathologic analyses

Samples of selected tissues (heart, biceps femoris, and diaphragm muscles) were frozen and sectioned (8 μm thick) for dystrophin immune-labeling and staining for visualization of connective tissue. Dystrophin/mini-dystrophin and connective tissue were visualized using the mouse monoclonal anti-dystrophin antibody NCL-DYSB (1:50, Novocastra Laboratories, Newcastle upon Tyne, UK) and Alexa Fluor 555 WGA conjugate (1:500, Molecular Probes, Eugene, OR,

USA), respectively. Nuclei were stained with DRAQ5 (1:1,000; BioStatus, Shepshed, UK). Heart sections were stained for collagen with picrosirius red F3B (Sigma-Aldrich Chimie, Lyon, France). Quantification of WGA-positive areas in biceps femoris and diaphragm sections and quantification of the dystrophin-positive fibers was performed using ImageJ open-source image processing software (v.2.0.0-rc-49/1.51a). To evaluate the robustness of dystrophin-positive fiber quantification, the results obtained using this approach were compared with those obtained manually (non-automated counting) in 6 biceps femoris samples. The absolute difference was less than 3.5% in all cases (mean, 2.4%).

Samples destined for histopathologic evaluation were embedded in paraffin wax within 48 h of collection, and 5-µm-thick sections were stained with hematoxylin and eosin saffron (HES).

Regenerative activity was assessed by detection of the developmental myosin heavy-chain isoform MyoHCDev in biceps femoris muscle samples from all rats using the NCL-MHCd antibody (Novocastra).

All histological analyses were conducted in a blinded manner by a qualified doctor of veterinary medicine who was a European board-certified pathologist.

Skeletal muscle function assessment
Grip test measurements were performed at the end of the study by an experimenter blind to genotype (WT or DMD^{mdx}) and treatment (vehicle or vector) using a grip meter (Bio-GT3, BIOSEB, France) attached to a force transducer. Rats were placed with their forepaws resting on a T-bar and were gently pulled backward until they released their grip.[34] The peak force generated was the first parameter measured. Then 5 consecutive grip strength tests were performed with a short (20–40 s) interval between each test, and the reduction in strength between the first and the last test was taken as an index of fatigue.

Cardiac muscle function assessment
Echocardiographic measurements were performed just before sacrifice. Anesthesia was induced with etomidate (Hypnomidate, 16 mg/kg, i.p.; Piramal Critical Care, West Drayton, UK) administered in 2 shots separated by 3 min. Two-dimensional echocardiography was performed using a Vivid 7 Dimension ultrasound machine (GE Healthcare) with a 14-MHz transducer. To detect possible structural remodeling, LV end-diastolic diameter and free-wall end-diastolic thickness were measured during diastole from long- and short-axis images obtained by M-mode echocardiography. Systolic function was assessed by measuring EF, whereas transmitral flow measurements of ventricular filling velocity were obtained using pulsed Doppler with an apical 4-chamber orientation. Diastolic dysfunction was assessed based on Doppler-derived E/A velocities, the E/A ratio, IVRT, and DT.

Evaluation of the immune responses
Anti-mini-dystrophin IgG antibodies were detected in sera from all study rats using a western blot-based assay. Briefly, optidys-3978-pos-

itive extracts were obtained after cell transfection (HEK293 cell line) using a plasmid encoding the optidys-3978 transgene under control of the cytomegalovirus promoter. Protein extracts from transfected and non-transfected HEK293 cells were subjected to electrophoresis using the NuPAGE Large Protein Blotting Kit (3%–8% Tris acetate precast polyacrylamide gel; Invitrogen, Carlsbad, CA, USA). Animal sera (pre-injection and at 3 or 6 months p.i.) were screened at dilution of 1/500. For each western blot membrane, the positive control consisted of a MANEX1011C mouse anti-dystrophin monoclonal antibody (Wolfson Center for Inherited Neuromuscular Disease, Oswestry, UK).

Circulating anti-AAV9 capsid IgG antibodies were detected using an enzyme-linked immunosorbent assay (ELISA). Rat serum samples (3 or 6 months p.i.) were tested at 6 dilutions (1/10, 1/40, 1/160, 1/2,560, and 1/10,240). The threshold of positivity of the assay was calculated for each dilution using 19 serum samples from naive rats harboring the same genetic background as mean of optical density (OD) for each dilution + 3 × SD. IgG titers for experimental animals were defined as the last serum dilution for which OD remained above the threshold.

Anti-AAV9 neutralizing factors (NFs) were detected at baseline and 3 and 6 months p.i. using a neutralization assay consisting of a cell transduction inhibition assay using an AAV9 vector expressing the lacZ reporter gene. Gene expression was measured using a luminometric method (Galacto-Star kit, Life Technologies, Thermo Fisher Scientific). Each serum was tested at a range of dilutions (1/50, 1/500, 1/5,000, 1/50,000 and 1/500,000). The cutoff of the assay was set up at 1/50. The NF titer was determined as the lowest dilution inhibiting cell transduction by more than 50% (with respect to levels of transduction observed with AAV9 alone).

The anti-mini-dystrophin and anti-AAV9 capsid T cell responses were monitored using an IFNγ ELISpot assay (rat-specific IFN-γ ELISpot BASIC Kit; Mabtech, Stockholm, Sweden). Splenocytes were harvested at 3 or 6 months p.i., and cell stimulation was performed using overlapping peptide pools (length of 15-mers, overlap of 10 amino acids) covering the entire sequences of either optidys-3978 protein or AAV9 capsid VP1 protein. For each experimental sample, negative and positive controls consisted of unstimulated cells (medium) and cells stimulated with mitogenic concanavalin A (ConA), respectively. Spot number was determined using an ELISpot reader ELR07 AID AutoImmun Diagnostika, Gmbh and analyzed with ELISpot Reader software v.7.0. (AID AutoImmun Diagnostika, Gmbh) Responses were considered positive when the number of spot-forming colonies (SFCs) per 1e6 cells was more than 50 and at least 3-fold higher than under the control condition. All the immune assays described above were performed by operators who were blinded to rat groups and treatments.

Statistical analysis
Statistical evaluation of data was performed using the non-parametric Kruskal-Wallis test to analyze differences between groups. Where significant overall effects were detected, differences between WT and DMD^{mdx} groups were assessed using Dunn's post hoc test. Repeated

grip force values were analyzed using the Friedman test, followed by Dunn's post hoc test.

SUPPLEMENTAL INFORMATION

Supplemental information can be found online at https://doi.org/10.1016/j.omtm.2023.05.017.

AUTHOR CONTRIBUTIONS

C.L.G., X.X., J.O., M.M., P.M., and R.J.S. designed the study and reviewed some or all of the primary data. X.X., J.G., J.L., and R.J.S. designed and constructed the vector. I.A. and S.R. provided DMD^{mdx} rats. C.L.G. performed and reviewed the molecular and biochemical analyses. T.L. performed and reviewed the histopathologic and immunochemistry analyses. V.F. and H.N. performed and reviewed the peptide immunoaffinity liquid chromatography-tandem mass spectrometry analysis. A.L., C.H., and G.T. performed and reviewed the clinical and physiological evaluations. O.A. performed and reviewed the immunologic analyses. All authors contributed to development of the manuscript and approved the final draft for submission.

DECLARATIONS OF INTERESTS

J.O., H.N., and V.F. are employees of and hold stock in Pfizer. C.L.G. and P.M. are co-authors of a patent for systemic treatment of dystrophic pathologies (EP3044319A1, dated June 27, 2014).

REFERENCES

1. Hoffman, E.P., Brown, R.H., Jr., and Kunkel, L.M. (1987). Dystrophin: the protein product of the Duchenne muscular dystrophy locus. Cell 51, 919–928. https://doi.org/10.1016/0092-8674(87)90579-4.

2. Mendell, J.R., and Lloyd-Puryear, M. (2013). Report of MDA muscle disease symposium on newborn screening for Duchenne muscular dystrophy. Muscle Nerve 48, 21–26. https://doi.org/10.1002/mus.23810.

3. Michele, D.E., and Campbell, K.P. (2003). Dystrophin-glycoprotein complex: posttranslational processing and dystroglycan function. J. Biol. Chem. 278, 15457–15460. https://doi.org/10.1074/jbc.R200031200.

4. Bogdanovich, S., Krag, T.O.B., Barton, E.R., Morris, L.D., Whittemore, L.A., Ahima, R.S., and Khurana, T.S. (2002). Functional improvement of dystrophic muscle by myostatin blockade. Nature 420, 418–421. https://doi.org/10.1038/nature01154.

5. Boland, B.J., Silbert, P.L., Groover, R.V., Wollan, P.C., and Silverstein, M.D. (1996). Skeletal, cardiac, and smooth muscle failure in Duchenne muscular dystrophy. Pediatr. Neurol. 14, 7–12. https://doi.org/10.1016/0887-8994(95)00251-0.

6. Koeks, Z., Bladen, C.L., Salgado, D., van Zwet, E., Pogoryelova, O., McMacken, G., Monges, S., Foncuberta, M.E., Kekou, K., Kosma, K., et al. (2017). Clinical outcomes in Duchenne muscular dystrophy: a study of 5345 patients from the TREAT-NMD DMD global database. J. Neuromuscul. Dis. 4, 293–306. https://doi.org/10.3233/JND-170280.

7. Werneck, L.C., Lorenzoni, P.J., Ducci, R.D.P., Fustes, O.H., Kay, C.S.K., and Scola, R.H. (2019). Duchenne muscular dystrophy: an historical treatment review. Arq. Neuropsiquiatr. 77, 579–589. https://doi.org/10.1590/0004-282X20190088.

8. McDonald, C.M., Henricson, E.K., Abresch, R.T., Duong, T., Joyce, N.C., Hu, F., Clemens, P.R., Hoffman, E.P., Cnaan, A., and Gordish-Dressman, H.; CINRG Investigators (2018). Long-term effects of glucocorticoids on function, quality of life, and survival in patients with Duchenne muscular dystrophy: a prospective cohort study. Lancet 391, 451–461. https://doi.org/10.1016/S0140-6736(17)32160-8.

9. Duan, D., Goemans, N., Takeda, S., Mercuri, E., and Aartsma-Rus, A. (2021). Duchenne muscular dystrophy. Nat. Rev. Dis. Primers 7, 13. https://doi.org/10.1038/s41572-021-00248-3.

10. Pascual-Morena, C., Cavero-Redondo, I., Álvarez-Bueno, C., Mesas, A.E., Pozuelo-Carrascosa, D., and Martínez-Vizcaíno, V. (2020). Restorative treatments of dystrophin expression in Duchenne muscular dystrophy: a systematic review. Ann. Clin. Transl. Neurol. 7, 1738–1752. https://doi.org/10.1002/acn3.51149.

11. Hashim, H.Z., Che Abdullah, S.T., Wan Sulaiman, W.A., Hoo, F.K., and Basri, H. (2014). Hunting for a cure: the therapeutic potential of gene therapy in Duchenne muscular dystrophy. Tzu Chi Med. J. 26, 5–9.

12. Büeler, H. (1999). Adeno-associated viral vectors for gene transfer and gene therapy. Biol. Chem. 380, 613–622. https://doi.org/10.1515/BC.1999.078.

13. Muzyczka, N. (1992). Use of adeno-associated virus as a general transduction vector for mammalian cells. Curr. Top. Microbiol. Immunol. 158, 97–129. https://doi.org/10.1007/978-3-642-75608-5_5.

14. Flotte, T.R. (2000). Size does matter: overcoming the adeno-associated virus packaging limit. Respir. Res. 1, 16–18. https://doi.org/10.1186/rr6.

15. Duan, D. (2018). Systemic AAV micro-dystrophin gene therapy for Duchenne muscular dystrophy. Mol. Ther. 26, 2337–2356. https://doi.org/10.1016/j.ymthe.2018.07.011.

16. Rodgers, B.D., Bishaw, Y., Kagel, D., Ramos, J.N., and Maricelli, J.W. (2020). Micro-dystrophin gene therapy partially enhances exercise capacity in older adult mdx Mice. Mol. Ther. Methods Clin. Dev. 17, 122–132. https://doi.org/10.1016/j.omtm.2019.11.015.

17. Harper, S.Q., Hauser, M.A., DelloRusso, C., Duan, D., Crawford, R.W., Phelps, S.F., Harper, H.A., Robinson, A.S., Engelhardt, J.F., Brooks, S.V., et al. (2002). Modular flexibility of dystrophin: implications for gene therapy of Duchenne muscular dystrophy. Nat. Med. 8, 253–261. https://doi.org/10.1038/nm0302-253.

18. Li, J., Sun, W., Wang, B., Xiao, X., and Liu, X.Q. (2008). Protein trans-splicing as a means for viral vector-mediated in vivo gene therapy. Hum. Gene Ther. 19, 958–964. https://doi.org/10.1089/hum.2008.009.

19. Phelps, S.F., Hauser, M.A., Cole, N.M., Rafael, J.A., Hinkle, R.T., Faulkner, J.A., and Chamberlain, J.S. (1995). Expression of full-length and truncated dystrophin minigenes in transgenic mdx mice. Hum. Mol. Genet. 4, 1251–1258. https://doi.org/10.1093/hmg/4.8.1251.

20. Sun, L., Li, J., and Xiao, X. (2000). Overcoming adeno-associated virus vector size limitation through viral DNA heterodimerization. Nat. Med. 6, 599–602. https://doi.org/10.1038/75087.

21. Wang, B., Li, J., and Xiao, X. (2000). Adeno-associated virus vector carrying human minidystrophin genes effectively ameliorates muscular dystrophy in mdx mouse model. Proc. Natl. Acad. Sci. USA 97, 13714–13719. https://doi.org/10.1073/pnas.240335297.

22. Yuasa, K., Ishii, A., Miyagoe, Y., and Takeda, S. (1997). [Introduction of rod-deleted dystrophin cDNA, delta DysM3, into mdx skeletal muscle using adenovirus vector]. Nihon Rinsho. 55, 3148–3153. https://www.ncbi.nlm.nih.gov/pubmed/9436426.

23. Shen, S., Bryant, K.D., Brown, S.M., Randell, S.H., and Asokan, A. (2011). Terminal N-linked galactose is the primary receptor for adeno-associated virus 9. J. Biol. Chem. 286, 13532–13540. https://doi.org/10.1074/jbc.M110.210922.

24. Wu, Z., Asokan, A., and Samulski, R.J. (2006). Adeno-associated virus serotypes: vector toolkit for human gene therapy. Mol. Ther. 14, 316–327. https://doi.org/10.1016/j.ymthe.2006.05.009.

25. DiMattia, M.A., Nam, H.J., Van Vliet, K., Mitchell, M., Bennett, A., Gurda, B.L., McKenna, R., Olson, N.H., Sinkovits, R.S., Potter, M., et al. (2012). Structural insight into the unique properties of adeno-associated virus serotype 9. J. Virol. 86, 6947–6958. https://doi.org/10.1128/JVI.07232-11.

26. Inagaki, K., Fuess, S., Storm, T.A., Gibson, G.A., McTiernan, C.F., Kay, M.A., and Nakai, H. (2006). Robust systemic transduction with AAV9 vectors in mice: efficient global cardiac gene transfer superior to that of AAV8. Mol. Ther. 14, 45–53. https://doi.org/10.1016/j.ymthe.2006.03.014.

27. Kornegay, J.N., Li, J., Bogan, J.R., Bogan, D.J., Chen, C., Zheng, H., Wang, B., Qiao, C., Howard, J.F., Jr., and Xiao, X. (2010). Widespread muscle expression of an AAV9 human mini-dystrophin vector after intravenous injection in neonatal dystrophin-deficient dogs. Mol. Ther. 18, 1501–1508. https://doi.org/10.1038/mt.2010.94.

28. Gregorevic, P., Allen, J.M., Minami, E., Blankinship, M.J., Haraguchi, M., Meuse, L., Finn, E., Adams, M.E., Froehner, S.C., Murry, C.E., et al. (2006). rAAV6-microdystrophin preserves muscle function and extends lifespan in severely dystrophic mice. Nat. Med. 12, 787–789. https://doi.org/10.1038/nm1439.

29. Le Guiner, C., Servais, L., Montus, M., Larcher, T., Fraysse, B., Moullec, S., Allais, M., François, V., Dutilleul, M., Malerba, A., et al. (2017). Long-term microdystrophin gene therapy is effective in a canine model of Duchenne muscular dystrophy. Nat. Commun. 8, 16105. https://doi.org/10.1038/ncomms16105.

30. Ramos, J.N., Hollinger, K., Bengtsson, N.E., Allen, J.M., Hauschka, S.D., and Chamberlain, J.S. (2019). Development of novel micro-dystrophins with enhanced functionality. Mol. Ther. 27, 623–635. https://doi.org/10.1016/j.ymthe.2019.01.002.

31. Wang, B., Li, J., Fu, F.H., and Xiao, X. (2009). Systemic human minidystrophin gene transfer improves functions and life span of dystrophin and dystrophin/utrophin-deficient mice. J. Orthop. Res. 27, 421–426. https://doi.org/10.1002/jor.20781.

32. Yue, Y., Pan, X., Hakim, C.H., Kodippili, K., Zhang, K., Shin, J.H., Yang, H.T., McDonald, T., and Duan, D. (2015). Safe and bodywide muscle transduction in young adult Duchenne muscular dystrophy dogs with adeno-associated virus. Hum. Mol. Genet. 24, 5880–5890. https://doi.org/10.1093/hmg/ddv310.

33. Caudal, D., François, V., Lafoux, A., Ledevin, M., Anegon, I., Le Guiner, C., Larcher, T., and Huchet, C. (2020). Characterization of brain dystrophins absence and impact in dystrophin-deficient DMDmdx rat model. PLoS One 15, e0230083. https://doi.org/10.1371/journal.pone.0230083.

34. Larcher, T., Lafoux, A., Tesson, L., Remy, S., Thepenier, V., François, V., Le Guiner, C., Goubin, H., Dutilleul, M., Guigand, L., et al. (2014). Characterization of dystrophin deficient rats: a new model for Duchenne muscular dystrophy. PLoS One 9, e110371. https://doi.org/10.1371/journal.pone.0110371.

35. Ouisse, L.H., Remy, S., Lafoux, A., Larcher, T., Tesson, L., Chenouard, V., Guillonneau, C., Brusselle, L., Vimond, N., Rouger, K., et al. (2019). Immunophenotype of a rat model of Duchenne's disease and demonstration of improved muscle strength after anti-CD45RC antibody treatment. Front. Immunol. 10, 2131. https://doi.org/10.3389/fimmu.2019.02131.

36. Szabó, P.L., Ebner, J., Koenig, X., Hamza, O., Watzinger, S., Trojanek, S., Abraham, D., Todt, H., Kubista, H., Schicker, K., et al. (2021). Cardiovascular phenotype of the DMD(mdx) rat - a suitable animal model for Duchenne muscular dystrophy. Dis. Model. Mech. 14, dmm047704. https://doi.org/10.1242/dmm.047704.

37. Egorova, T.V., Galkin, I.I., Ivanova, Y.V., and Polikarpova, A.V. (2021). Duchenne muscular dystrophy animal models. In Animal Models in Medicine and Biology, E. Purevjav, J.F. Pierre, and L. Lu, eds.. https://doi.org/10.5772/intechopen96738, https://www.intechopen.com/online-first/75702.

38. Farrokhi, V., Walsh, J., Palandra, J., Brodfuehrer, J., Caiazzo, T., Owens, J., Binks, M., Neelakantan, S., Yong, F., Dua, P., et al. (2022). Dystrophin and mini-dystrophin quantification by mass spectrometry in skeletal muscle for gene therapy development in Duchenne muscular dystrophy. Gene Ther. 29, 608–615. https://doi.org/10.1038/s41434-021-00300-7.

39. Kostrominova, T.Y. (2011). Application of WGA lectin staining for visualization of the connective tissue in skeletal muscle, bone, and ligament/tendon studies. Microsc. Res. Tech. 74, 18–22. https://doi.org/10.1002/jemt.20865.

40. Rodríguez-Cruz, M., Almeida-Becerril, T., Atilano-Miguel, S., Cárdenas-Conejo, A., and Bernabe-García, M. (2020). Natural history of serum enzyme levels in Duchenne muscular dystrophy and implications for clinical practice. Am. J. Phys. Med. Rehabil. 99, 1121–1128. https://doi.org/10.1097/PHM.0000000000001500.

41. Wang, M., Sun, J., Crosby, A., Woodard, K., Hirsch, M.L., Samulski, R.J., and Li, C. (2017). Direct interaction of human serum proteins with AAV virions to enhance AAV transduction: immediate impact on clinical applications. Gene Ther. 24, 49–59. https://doi.org/10.1038/gt.2016.75.

42. Mingozzi, F., Meulenberg, J.J., Hui, D.J., Basner-Tschakarjan, E., Hasbrouck, N.C., Edmonson, S.A., Hutnick, N.A., Betts, M.R., Kastelein, J.J., Stroes, E.S., et al. (2009). AAV-1-mediated gene transfer to skeletal muscle in humans results in dose-dependent activation of capsid-specific T cells. Blood 114, 2077–2086. https://doi.org/10.1182/blood-2008-07-167510.

43. Nathwani, A.C., Tuddenham, E.G.D., Rangarajan, S., Rosales, C., McIntosh, J., Linch, D.C., Chowdary, P., Riddell, A., Pie, A.J., Harrington, C., et al. (2011). Adenovirus-associated virus vector-mediated gene transfer in hemophilia B. N. Engl. J. Med. 365, 2357–2365. https://doi.org/10.1056/NEJMoa1108046.

44. Nakamura, K., Fujii, W., Tsuboi, M., Tanihata, J., Teramoto, N., Takeuchi, S., Naito, K., Yamanouchi, K., and Nishihara, M. (2014). Generation of muscular dystrophy model rats with a CRISPR/Cas system. Sci. Rep. 4, 5635. https://doi.org/10.1038/srep05635.

45. Creisméas, A., Gazaille, C., Bourdon, A., Lallemand, M.A., François, V., Allais, M., Ledevin, M., Larcher, T., Toumaniantz, G., Lafoux, A., et al. (2021). TRPC3, but not TRPC1, as a good therapeutic target for standalone or complementary treatment of DMD. J. Transl. Med. 19, 519. https://doi.org/10.1186/s12967-021-03191-9.

46. Huchet, C., Toumaniantz, G., Larcher, T., Fraysse, B., Lafoux, A., Remy, S., Caudal, D., Allais, M., Amosse, E., Anegon, I., and Guiner, C.L. (2017). Exhaustive characterization of the newly developed Duchenne muscular dystrophy rat model: a unique animal model for DMD which mimics the human disease at both the muscular and the cardiac levels. Neuromuscul. Dis. 27, S247.

47. McGreevy, J.W., Hakim, C.H., McIntosh, M.A., and Duan, D. (2015). Animal models of Duchenne muscular dystrophy: from basic mechanisms to gene therapy. Dis. Model. Mech. 8, 195–213. https://doi.org/10.1242/dmm.018424.

48. Emery, A.E.H., and Muntoni, F. (2003). Duchenne Muscular Dystrophy, 3rd ed. (Oxford: Oxford University Press).

49. Pulicherla, N., Shen, S., Yadav, S., Debbink, K., Govindasamy, L., Agbandje-McKenna, M., and Asokan, A. (2011). Engineering liver-detargeted AAV9 vectors for cardiac and musculoskeletal gene transfer. Mol. Ther. 19, 1070–1078. https://doi.org/10.1038/mt.2011.22.

50. Bish, L.T., Morine, K., Sleeper, M.M., Sanmiguel, J., Wu, D., Gao, G., Wilson, J.M., and Sweeney, H.L. (2008). Adeno-associated virus (AAV) serotype 9 provides global cardiac gene transfer superior to AAV1, AAV6, AAV7, and AAV8 in the mouse and rat. Hum. Gene Ther. 19, 1359–1368. https://doi.org/10.1089/hum.2008.123.

51. Fang, H., Lai, N.C., Gao, M.H., Miyanohara, A., Roth, D.M., Tang, T., and Hammond, H.K. (2012). Comparison of adeno-associated virus serotypes and delivery methods for cardiac gene transfer. Hum. Gene Ther. Methods 23, 234–241. https://doi.org/10.1089/hgtb.2012.105.

52. Zincarelli, C., Soltys, S., Rengo, G., and Rabinowitz, J.E. (2008). Analysis of AAV serotypes 1-9 mediated gene expression and tropism in mice after systemic injection. Mol. Ther. 16, 1073–1080. https://doi.org/10.1038/mt.2008.76.

53. Pan, X., Yue, Y., Zhang, K., Hakim, C.H., Kodippili, K., McDonald, T., and Duan, D. (2015). AAV-8 is more efficient than AAV-9 in transducing neonatal dog heart. Hum. Gene Ther. Methods 26, 54–61. https://doi.org/10.1089/hgtb.2014.128.

54. Butterfield, R., Shieh, P., Yong, F., Binks, M., McDonnell, T.G., Ryan, K.A., Belluscio, B., Neelakantan, S., Levy, D., Schwartz, P.F., et al. (2022). One year data from ambulatory boys in a phase 1B, open-label study of fordadistrogene movaparvovec (PF-06939926) for Duchenne muscular dystrophy (DMD). In Presented at the Muscular Dytsrophy Association Clinical & Scientific Conference, March 13-16, 2022, Nashville, TN, https://mdaconference.org/node/1566.

55. Belluscio, B., Beaverson, K., Garnier, N., Ryan, K., Moorehead, T., Yong, F., and Binks, M. (2021). Safety and efficacy of PF-06939926 gene therapy in boys with Duchenne muscular dystrophy: update on data from the phase 1B study. In Paper Presented at the Muscular Dystrophy Association (MDA) Clinical and Scientific Conference.

56. Clément, N., and Grieger, J.C. (2016). Manufacturing of recombinant adeno-associated viral vectors for clinical trials. Mol. Ther. Methods Clin. Dev. 3, 16002. https://doi.org/10.1038/mtm.2016.2.

57. Le Guiner, C., Moullier, P., and Arruda, V.R. (2011). Biodistribution and shedding of AAV vectors. Methods Mol. Biol. 807, 339–359. https://doi.org/10.1007/978-1-61779-370-7_15.